Acoustic modal expansion of open cavity using coupled mode theory

Yuhui Tong, Yiwei Kou, Jie Pan

April 23, 2016

Schoold of Mechanical and Chemical Engineering, The University of Western Australia, Crawley, WA 6009, Australia

1 Introduction

Open cavity widely ... problem

Intensive study eigenvalue problem, the modal expansion has long been absence.

Several attempts done before, but none solve the problem nor did provide any information to verify the ...

A recent progress made in acoustic resonators for using coupled mode theory, to . It is also proved that with frequency-dependent eigenmodes.

In the present paper, it is extended to open cavity problem. The baffled being treated ...

2 Theory

2.1 Phase I, problem formulation

As depicted in Fig. 1, the rectangular cavity with an opening located at an infinite baffle is investigated in the present paper. For the sake of simplicity, all boundaries are rigid.

The sound pressure (omitting the time dependence $e^{j\omega t}$) excited by a monopole source inside the cavity can be obtained by solving the inhomogeneous Helmholtz equation

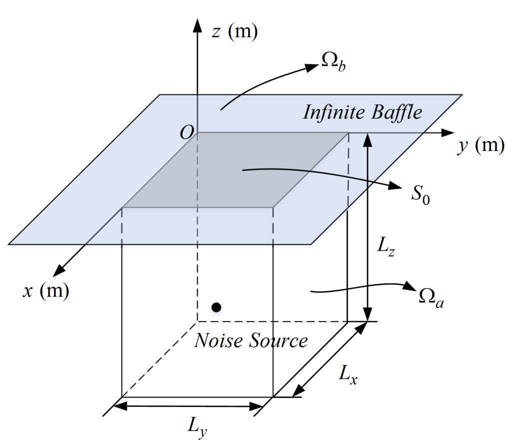

Figure 1: A schematic diaggram of an baffled open cavity.

$$\nabla^2 p + k^2 p = -q_s \delta(\boldsymbol{x} - \boldsymbol{x}_s), \tag{1}$$

where $k = \omega/c_0$ is the wavenumber, q_s is the source strength, $\boldsymbol{x}_s$ is the position of the monopole source, which is supposed to be within the cavity. The solution of Eq. (1) can be written respectively for cavity area Ω_a, and upper half space Ω_b. For Ω_a,

$$p_a(\boldsymbol{x}) = \sum_{\mu,\nu,\xi} a_{\mu,\nu,\xi} \phi_{\mu,\nu,\xi}(\boldsymbol{x}), \tag{2}$$

where $\phi_{\mu',\nu',\xi'}(\boldsymbol{x}) = \psi_{\mu'}(x)\psi_{\nu'}(y)\psi_{\xi'}(z)$ is the eigenmode for *enclosed* cavity and $\psi_m(x) = \sqrt{\frac{2-\delta_{0,m}}{L_x}} \cos(\frac{m\pi}{L_x}x)$. For Ω_b,

$$p_b(\boldsymbol{x}) = jk\rho c \iint_{S_0} G_b(\boldsymbol{x}, \boldsymbol{x}') v_\perp(\boldsymbol{x}') dS', \tag{3}$$

where $G_b(\boldsymbol{x}, \boldsymbol{x}') = \frac{1}{2\pi} \frac{e^{-jk|\boldsymbol{x}-\boldsymbol{x}'|}}{|\boldsymbol{x}-\boldsymbol{x}'|}$ is the Green's function for the upper half space, $v_\perp(\boldsymbol{x}')$ is the normal velocity distribution at the opening S_0 (the intersection between Ω_a and Ω_b), the integral is invaluated over S_0.

In Ω_a, p_a satisfies,

$$\nabla^2 p_a(\boldsymbol{x}) + k^2 p_a(\boldsymbol{x}) = -q_s \delta(\boldsymbol{x} - \boldsymbol{x}_s), \tag{4}$$

together with corresponding boundary conditions, while $\phi_{\mu,\nu,\xi}$ satisfies,

$$\nabla^2 \phi_{\mu,\nu,\xi} + k^2_{\mu,\nu,\xi} \phi_{\mu,\nu,\xi} = 0, \tag{5}$$
$$k^2_{\mu,\nu,\xi} = (\mu\pi/L_x)^2 + (\nu\pi/L_y)^2 + (\xi\pi/L_z)^2,$$

and rigid boundary condition for all six walls of the rectangular cavity, including S_0. Multiplying Eq. (4) and Eq. (5) by $\phi_{\mu,\nu,\xi}$ and p_a respectively and taking the difference of the resulting equations yields,

$$\left(p_a \nabla^2 \phi_{\mu,\nu,\xi} - \phi_{\mu,\nu,\xi} \nabla^2 p_a\right) + (k^2_{\mu,\nu,\xi} - k^2) p_a \phi_{\mu,\nu,\xi} = q_s \phi_{\mu,\nu,\xi} \delta(\boldsymbol{x} - \boldsymbol{x}_s). \tag{6}$$

Integrating over Ω_a and applying Green's theorem gives

$$jk\rho c \iint_{S_0} \phi_{\mu,\nu,\xi} v_\perp dS_0 + (k^2_{\mu,\nu,\xi} - k^2) a_{\mu,\nu,\xi} = q_0 \phi_{\mu,\nu,\xi}(\boldsymbol{x}_s). \tag{7}$$

The above equation can be further simplied into

$$\sum_{m,n} jk \psi_\xi(0) \delta_{\mu,m} \delta_{\nu,n} \rho_0 c_0 V_{m,n} + (k^2_{\mu,\nu,\xi} - k^2) a_{\mu,\nu,\xi} = q_0 \phi_{\mu,\nu,\xi}(\boldsymbol{x}_s), \tag{8}$$

by noting the expansion of $v_\perp(x, y)$

$$v_\perp(x, y) = \sum_{m,n} V_{m,n} \psi_m(x) \psi_n(y). \tag{9}$$

Another constraint is the continuity condition for sound pressure at the interface, i.e., $p_a|_{S_0} = p_b|_{S_0}$ such that

$$\sum_{\mu',\nu',\xi'} a_{\mu',\nu',\xi'} \psi_{\mu'}(x) \psi_{\nu'}(y) \psi_{\xi'}(0) = jk\rho c \iint_{S_0} \frac{e^{-jk\sqrt{(x-x')^2+(x-y')^2}}}{2\pi\sqrt{(x-x')^2+(x-y')^2}} \sum_{m,n} V_{m,n} \psi_m(x') \psi_n(y') dS_0 \tag{10}$$

Multiplying $\psi_\mu(x)\psi_\nu(y)$ and integrate over the interface leads to,

$$\sum_{\mu',\nu',\xi'} \delta_{\mu,\mu'}\delta_{\nu,\nu'}\psi_{\xi'}(0)a_{\mu',\nu',\xi'} = \rho_0 c_0 \sum_{m,n} Z_{\mu,\nu,m,n}V_{m,n}, \tag{11}$$

where $Z_{\mu,\nu,m,n}$ is the radiation impedance of an baffled rectangular plate of $L_x \times L_y$

$$Z_{\mu,\nu,m,n} = jk \iint_{S_0} \iint_{S_0} \psi_\mu(x)\psi_\nu(y) \frac{e^{-jk\sqrt{(x-x')^2+(x-y')^2}}}{2\pi\sqrt{(x-x')^2+(x-y')^2}} \psi_m(x')\psi_n(y')dS'dS \tag{12}$$

Using Eqs. (8) and (11), vectors $\boldsymbol{a} = \begin{bmatrix} \cdots & a_{\mu,\nu,\xi} & \cdots \end{bmatrix}^T$ and $\boldsymbol{V} = \begin{bmatrix} \cdots & V_{m,n} & \cdots \end{bmatrix}^T$ can be determined by solving

$$\boldsymbol{HV} + (\boldsymbol{K} - k^2\boldsymbol{I})\boldsymbol{a} = \boldsymbol{S} \tag{13}$$

$$\boldsymbol{Ma} = \boldsymbol{ZV} \tag{14}$$

where corresponding matrices are defined as follows: $\boldsymbol{H}_{(\mu,\nu,\xi),(m,n)} = jk\delta_{\mu,m}\delta_{\nu,n}\psi_\xi(0)$, $\boldsymbol{K}_{(\mu,\nu,\xi),(\mu',\nu',\xi')} = k^2_{\mu,\nu,\xi}\delta_{\mu,\mu'}\delta_{\nu,\nu'}\delta_{\xi,\xi'}$, $\boldsymbol{S} = q_s \begin{bmatrix} \cdots & \phi_{\mu,\nu,\xi}(\boldsymbol{x}_s) & \cdots \end{bmatrix}^T$, $\boldsymbol{M}_{(m,n),(\mu,\nu,\xi)} = \delta_{\mu,\mu'}\delta_{\nu,\nu'}\psi_{\xi'}(0)$, $\boldsymbol{Z}_{(\mu,\nu),(m,n)} = Z_{\mu,\nu,m,n}$. Eqs. (13) and (14) can be further reduced as

$$(\boldsymbol{D} - \boldsymbol{k^2})\boldsymbol{a} = \boldsymbol{S}, \tag{15}$$

where $\boldsymbol{D} = \boldsymbol{K} - \boldsymbol{HZ}^{-1}\boldsymbol{M}$ is known as effective Hamiltonian (reduced differential operator) on quantum physics.

2.2 Phase II Bi-orthogonal basis and modal expansion.

Eq. (15) gives rise to the following eigenvalue problem

$$\boldsymbol{D}\boldsymbol{g}_{\mu,\nu,\xi} = K^2_{\mu,\nu,\xi}\boldsymbol{g}_{\mu,\nu,\xi}, \tag{16}$$

where $K^2_{\mu,\nu,\xi}$ is the eigenvalue and the eigenvector $\boldsymbol{g}_{\mu,\nu,\xi}$ satisfies the bi-orthogonal relation

$$\boldsymbol{g}^T_{\mu',\nu',\xi'}\boldsymbol{g}_{\mu,\nu,\xi} = \delta_{\mu',\mu}\delta_{\nu,\nu'}\delta_{\xi,\xi'}\boldsymbol{g}^T_{\mu,\nu,\xi}\boldsymbol{g}_{\mu,\nu,\xi}. \tag{17}$$

An alternative expression of Eq. (17) is written as,

$$\iiint_{V_0} \Phi_{\mu',\nu',\xi'}(\boldsymbol{x})\Phi_{\mu,\nu,\xi}(\boldsymbol{x})dV = \delta_{\mu',\mu}\delta_{\nu,\nu'}\delta_{\xi,\xi'} \iiint_{V_0} \Phi^2_{\mu,\nu,\xi}(\boldsymbol{x})dV, \tag{18}$$

where $\Phi_{\mu,\nu,\xi}(\boldsymbol{x})$ is the modal function corresponding to $\boldsymbol{g}_{\mu,\nu,\xi}$ such that

$$\Phi_{\mu,\nu,\xi}(\boldsymbol{x}) = \sum_{\mu',\nu',\xi'} \left(\boldsymbol{g}_{\mu,\nu,\xi}\right)_{\mu',\nu',\xi'} \phi_{\mu',\nu',\xi'}(\boldsymbol{x}). \tag{19}$$

Expanding $\boldsymbol{a}$ into $\{\boldsymbol{g}_{\mu,\nu,\xi}\}$

$$\boldsymbol{a} = \sum_{\mu',\nu',\xi'} c_{\mu',\nu',\xi'}\boldsymbol{g}_{\mu',\nu',\xi'} \tag{20}$$

and making the substitution into Eq. (15) yields

$$c_{\mu,\nu,\xi} = \frac{\boldsymbol{g}^T_{\mu,\nu,\xi}\boldsymbol{S}}{(K^2_{\mu,\nu,\xi} - k^2)\boldsymbol{g}^T_{\mu,\nu,\xi}\boldsymbol{g}_{\mu,\nu,\xi}}. \tag{21}$$

Combining Eq. (20) together with Eqs. (2 ,3,14) leads to the modal expansion of sound pressure of the open cavity,

$$p(\boldsymbol{x}) = \begin{pmatrix} p_a(\boldsymbol{x}) \\ p_b(\boldsymbol{x}) \end{pmatrix} = \sum_{\mu,\nu,\xi} c_{\mu,\nu,\xi} \begin{pmatrix} \Phi_{\mu,\nu,\xi}(\boldsymbol{x}) \\ \Psi_{\mu,\nu,\xi}(\boldsymbol{x}) \end{pmatrix},$$

where $\Psi_{\mu,\nu,\xi}(\boldsymbol{x})$ is given by

$$\Psi_{\mu,\nu,\xi}(\boldsymbol{x}) = \boldsymbol{\varphi}^T \boldsymbol{Z}^{-1} \boldsymbol{M} \boldsymbol{g}_{\mu,\nu,\xi}.$$

Noted $\boldsymbol{\varphi} = \begin{bmatrix} \cdots & \varphi_{m,n}(\boldsymbol{x}) & \cdots \end{bmatrix}$, $\varphi_{m,n}(\boldsymbol{x}) = jk\rho c \iint_{S_0} G_b(\boldsymbol{x}, \boldsymbol{x}')\psi_m(x')\psi_n(y')dS'$ is the sound pressure induced by velocity distribution $\psi_m(x')\psi_n(y')$ on S_0.

3 Numerical validation

The theoretical results obtained in Sec. 2 is check numerically here. The cavity in Fig. 1 has the dimensions of 0.432m long (L_x), 0.67m wide (L_y) and 0.598m high (L_z), which was considered in literature (Wang). The source is located at $(0.1,\ 0.1,\ -L_z + 0.1)$ m with . The field points inside and outside the cavity are randomly chosen at $(0.2,\ 0.3,\ -L_z + 0.4)$ m and $(1.3,\ 1.4,\ -L_z + 1.5)$ m. The analytical method proposed in Sec. 2 is obtained with MATLAB codes, when 140 *closed* cavity modes are used for computation of eigensolutions to Eq. (16).

140 eigenmodes are obtained by analytical method for open rectangular cavity. Table. 1 lists the first 15 eigen solutions when noise frequency $f = 500$ Hz ($k = 9.24$), in constrast with the counterparts of closed cavity. It's clear that the eigenfrequencies of acoustic modes become complex in which the imaginary part corresponds to radiation loss. Table. 2 plots slices of $|\Psi_{\mu,\nu,\xi}|$, the modulus of modal function of (μ, ν, ξ) eigenmode. The nodal lines are distinguishable for these low frequency eigenmodes, which justifies the inheritance of the closed cavity modes' indexes μ, ν, ξ to classify the open cavity modes. The bi-orthogonality of the eigensolutions is checked in Tab. 3. Figure. 3 presents the amplitude each eigenmodes upon the monopole source with strength $q_s = jk\rho_0 c_0 q_0$, and $q_0 = 10^{-4} m^3/s$ where one can see that $|c_{\mu,\nu,\xi}|$ decays rapidly as the order of modes grows. $|c_{\mu,\nu,\xi}|$ takes the maximum value at (1,1,0) mode, of which the eigenfrequency takes $484.95 + 1.83j$ Hz. It is then checked the number of eigenmodes needed for calculation. Figure. 2 indicates less than 15 eigenmodes is necessary for sound pressure to converge at the probe points inside the cavity, while less than 20 eigenmodes for probe points outside the cavity. This result is quite reasonable considering the resonant eigenmode is the 6^{th} one.

The performance of the proposed method is then verified by calculating the sound pressure at field points inside and outside cavity for multiple frequencies below 500 Hz, where 20 eigenmodes will be used for calculation. The The reference result is obtain via finite element software COMSOL, where perfectly matched layers (PMLs) are used to model the semi-infinite space above the baffle. Noted only frequencie above 30 Hz are treated in COMSOL, as at very low frequency, the PMLs needed for calculation become so thick to prevent reflected wave. The source strength is taken as $q_s = 4\pi \times 10^{-4} kg/s^2$. Figure. 4 plots the comparison between results obtained by both methods, where excellent agreement suggests the

4 Conclusions and discussion

Acknowledgement

μ	ν	ξ	$f_{\mu,\nu,\xi}$ (Hz)	$F_{\mu,\nu,\xi}$ (Hz)
0	0	0	0	133.26+23.55j
0	1	0	253.73	283.08+8.64j
0	0	1	284.28	382.88+71.04j
0	1	1	381.04	449.37+40.02j
1	0	0	393.51	413.08+3.68j
1	1	0	468.22	484.95+1.83j
1	0	1	485.46	544.96+20.79j
0	2	0	507.46	522.01+2.07j
1	1	1	547.77	603.52+11.06j
0	0	2	568.56	604.31+75.40j
0	2	1	581.66	631.25+11.13j
0	1	2	622.60	666.71+46.10j
1	2	0	642.16	655+0.40j
1	0	2	691.46	743.95+28.66j
1	2	1	702.03	752.1+3.30j

Table 1: The first 15 modes of closed and open rectangular cavity, and the corresponding frequencies. $f_{\mu,\nu,\xi} = k_{\mu,\nu,\xi}c_0/2\pi$ for closed cavity; $F_{\mu,\nu,\xi} = K_{\mu,\nu,\xi}c_0/2\pi$ for open cavity, at source frequency $f = 500Hz$.

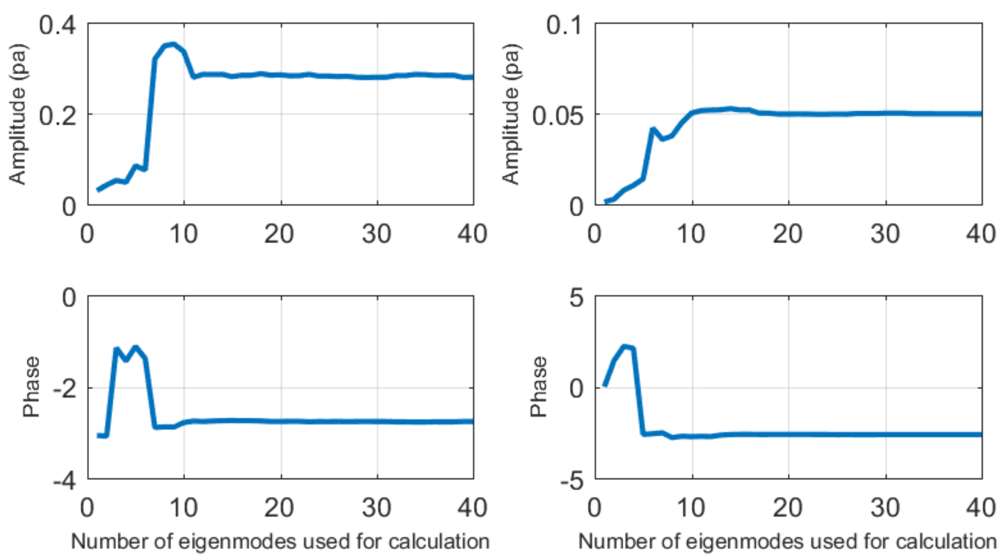

Figure 2: The calculated amplitude and phase of the sound pressure as a function of eigenmodes orders. The sound source is located at $(0.1,\ 0.1,\ -L_z+0.1)$ m with $f = 500Hz$, $q_s = 10^{-4}kg/s^2$; (left) location $(0.2,\ 0.3,\ -L_z+0.4)$ m in the cavity and (right) location $(1.3,\ 1.4,\ -L_z+1.5)$ m outside the cavity.

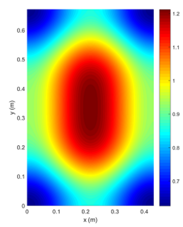

(0,0,0) mode $z = 0$ plane

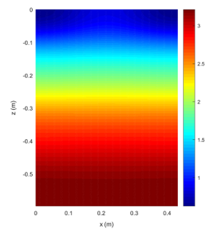

(0,0,0) mode $y = 0$ plane

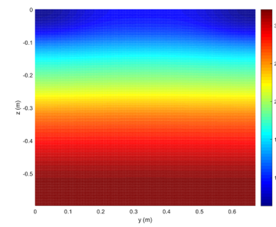

(0,0,0) mode $x = 0$ plane

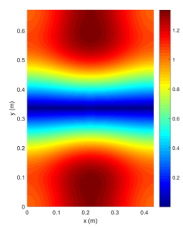

(0,1,0) mode $z = 0$ plane

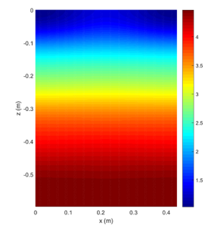

(0,1,0) mode $y = 0$ plane

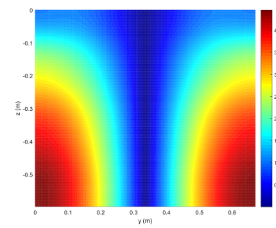

(0,1,0) mode $x = 0$ plane

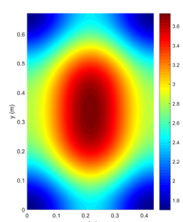

(0,0,1) mode $z = 0$ plane

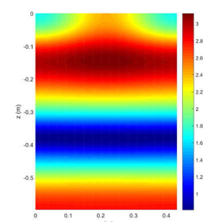

(0,0,1) mode $y = 0$ plane

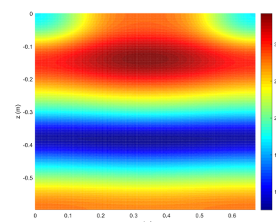

(0,0,1) mode $x = 0$ plane

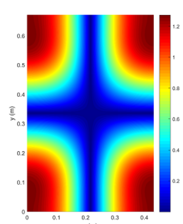

(1,1,0) mode $z = 0$ plane

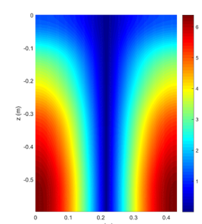

(1,1,0) mode $y = 0$ plane

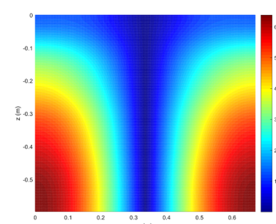

(1,1,0) mode $x = 0$ plane

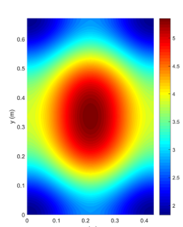

(0,0,2) mode $z = 0$ plane

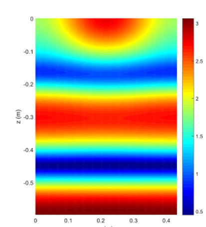

(0,0,2) mode $y = 0$ plane

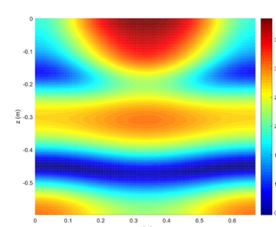

(0,0,2) mode $x = 0$ plane

Table 2: The modulus of $\Psi_{\mu,\nu,\xi}(\boldsymbol{x})$ for (0,0,0), (0,1,0), (0,0,1), (1,1,0), (0.0,2) modes, when source frequency $f = 500$ Hz.

	1	2	3	4
1	1	0	0	0
2	0	1	0	0
3	0	0	1	0
4	0	0	0	1

Table 3: The bi-orthogonality of first 4 modes.

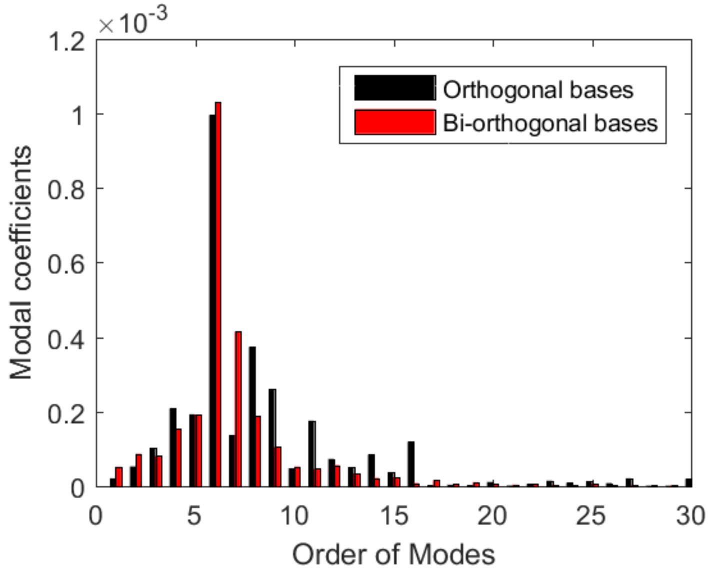

Figure 3: The amplitude of modal coefficients $|c_{\mu,\nu,\xi}|$, vs orders of mode, when source frequency is $500Hz$.

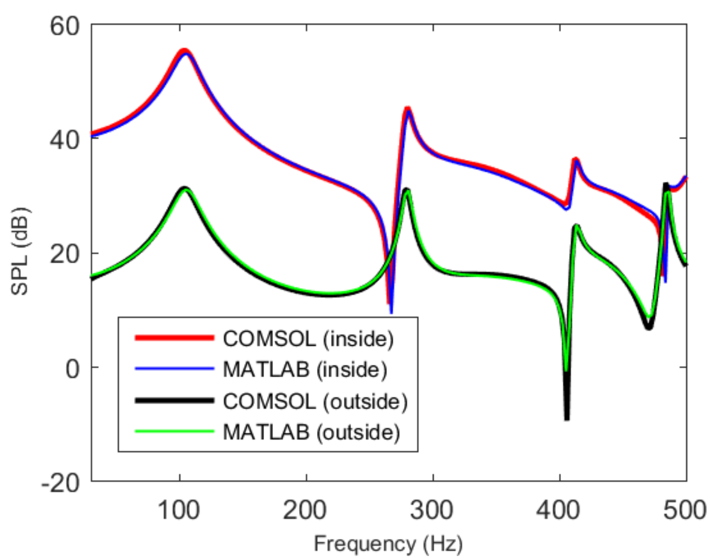

Figure 4: Comparison between the sound field obtained by the anlytical model (marked by MATLAB) and numerical simulations (marked by COMSOL) when the excitation point source is located at (0.1,0.1,0.1) m and $q0 = 10^{-4} m^3/s$; (a) sound pressure level at (0.2,0.3,0.4) m in the cavity and (1.3,1.4,1.5) m outside the cavity.